PFG 2014 / 4, 0275–0285
Stuttgart, August 2014

Article

The Effect of Vegetation Type and Density on X-Band SAR Backscatter after Forest Fires

Eva-Maria Bernhard, André Twele & Sandro Martinis, Oberpfaffenhofen

Keywords: forest fire, TerraSAR-X, backscatter analysis, change detection

Summary: Various frequencies, e.g. visible light, infrared, and microwaves, from remote sensing sensors can be used for active fire mapping, forest fire detection and fire emission assessment. However, little is known about the applicability of X-band SAR data for burned area detection. This paper presents a detailed SAR backscatter coefficient analysis and accuracy assessment with respect to CORINE 2006 land cover data. For this purpose five forest fires have been analysed. Dry as well as wet acquisition conditions have been taken into account. The analysis demonstrated that the largest differences in backscatter coefficients between pre- and post-fire conditions were linked to tall and dense vegetation types. Contrarily, scant vegetation was marked by lowest signal differences. High correlation coefficients have been obtained from regression analysis between vegetation indices and SAR backscatter changes. Moreover, a burned area classification algorithm with different thresholds for each vegetation type has been applied. The classification result illustrated that areas abundantly covered with vegetation showed classification accuracies of ~91%, whereas sparse vegetation achieved ~5% accuracies.

Zusammenfassung: *Der Einfluss von Vegetationstyp und -dichte auf das Rückstreuverhalten von X-Band Radar nach Waldbränden*. Verschiedene Frequenzen, z.B. sichtbares Licht, Infrarot und Mikrowellen, von Fernerkundungssensoren können zur Feuererfassung, der Brandflächendetektion oder zur Abschätzung von Emissionen genutzt werden. Allerdings ist nur wenig über die Eignung von X-Band Radardaten zur Brandflächendetektion bekannt. Daher präsentiert diese Studie eine detaillierte Analyse des Radar Rückstreuverhaltens über diversen Landbedeckungen (nach CORINE 2006). Fünf verschiedene Gebiete sind unter unterschiedlichen Witterungsbedingungen (trocken und nass) untersucht worden. Die Studie zeigt, dass die größten Unterschiede der Rückstreukoeffizienten – vor und nach dem Brandereignis – in Gebieten mit hochwachsender und dichter Vegetation auftreten, wohingegen Gebiete mit spärlicher Vegetation nur geringe Unterschiede aufweisen. Ebenso erzielen die Regressionskoeffizienten zwischen Vegetationsindizes und der Veränderung des Radar Rückstreusignals hohe Übereinstimmungen. Darüber hinaus wurde ein Klassifikationsalgorithmus für Brandflächen angewandt, der auf individuellen Schwellwerten für jeden Vegetationstyp basiert. Die Klassifikationsergebnisse zeigten, dass dicht bewachsene Gebiete Klassifikationsgenauigkeiten von bis zu 91% aufwiesen, wohingegen spärlich bewachsene Bereiche Klassifikationsgenauigkeiten von 5% erreichten.

1 Introduction

Forest fires have always been a natural component of the Mediterranean ecosystem regulating the evolution, productivity and biodiversity of vegetation (Margaris et al. 1996, Viegas et al. 2009). Nevertheless, the European Mediterranean region has suffered from an increasing number of large fire events (Justice & Koronzti 2001). These trends of environmental disasters are due to climate change and socio economic changes expected to continue and intensify in future (Justice & Koronzti 2001, Leone 2009, Wastl et al. 2012). On the contrary, an increase in the construction of wildland urban interfaces, the devel-

DOI: 10.1127/1432-8364/2014/0222 1432-8364/14/0222 $ 2.75

opment of tourist infrastructure and pressure from tourism activities amplify the risk of man-induced fires (Viegas et al. 2009). As a consequence, the role of burned area detection and post fire monitoring are of eminent importance to support fire fighters on site and quantify environmental damage of the ecosystem. Spaceborne remote sensing can contribute to pre-, active and post-disaster mapping with an almost global coverage. While mainly medium resolution optical or thermal sensors, e.g. MODIS and MSG-SEVIRI, are being used for active fire detection (Justice et al. 2002, Amraoui et al. 2010), burned area mapping can be performed with high and very high resolution imaging techniques. However, the applicability of optical data can be severely limited due to persistent cloud coverage, haze or smoke plumes. An alternative method for burned area detection lies in the use of synthetic aperture radar (SAR) data where measurements in the microwave regime can overcome the reported problems. Several studies have been carried out in boreal forests using C-band SAR data (Kasischke et al. 1992, French et al. 1996, Bourgeau-Chavez et al. 1997, Bourgeau-Chavez et al. 2002). In addition, the impact of different forest types on burned area detection have been studied for tropical rain forests (Siegert & Rücker 2000), wetlands (marshes and forest mix) (Karszenbaum et al. 2003), or savanna woodlands (Menges et al. 2004). These studies found evidence for a change in backscatter signal (C-, L-, and P-band data) between burned and unburned areas, mainly influenced by soil moisture and the exposure of a rough ground surface. Only few studies were undertaken in the European Mediterranean semi-arid environment, where precipitation during the fire season is rare, and the lack of rain reduces backscatter variability due to changes in soil moisture (Tanase et al. 2010a). Promising results could be achieved using C-band SAR data for burned area detection (Gimeno et al. 2003, Gimeno et al. 2004a, Gimeno et al. 2004b). The burned areas were distinguishable regardless of rainfall, although the wet season showed higher backscatter values than the dry season. Tanase et al. (2010a, 2010b, 2010c) confirmed the utility of X-, C-, and L- band data for fire severity assessment in dry and wet environmental conditions. Moreover, Bernhard et al. (2011) confirmed the detection capabilites of X-band SAR data for burned area mapping. This analysis was undertaken in La Palma and Grammatico, and indicated that the backscatter coefficient could be influenced by pre-fire vegetation. Since X-band microwaves cannot penetrate as deeply into vegetation cover as C-, L- or P-band, the incident beam interacts to a large extent with tree crowns (Hoekmann et al. 1987). The attenuation through the forest canopy depends on stand density, canopy architecture (like crown closure, crown shape) and the incidence angle of the sensor (Hoekmann et al. 1987). Pulliainen et al. (1993) showed that the transmissivity of X-band backscatter decreases nearly exponentially with increasing stem volume, whereas the soil backscatter contribution decreases (almost linearly) with stem volume. This indicates that the magnitude of backscatter changes after forest fires could be related to pre-fire vegetation characteristics.

This study substantially extends and complements the previous findings (Bernahrd et al. 2011) by taking additional study sites, i.e. Alto Trans-os-Montes, Dos Aguas and Andilla, into account, enhancing the classification algorithm and investigating in more detail the influence of pre-fire vegetation type and density on backscatter coefficients and classification results. Further, the data used in this study are acquired under dry and wet environmental conditions, which allowed determining SAR backscatter behaviour not only with respect to the vegetation structure, but also with respect to the impact of precipitation.

2 Study Sites

Five different study sites – the Canary Island of La Palma (Spain), Alto Trans-os-Montes (Portugal), Dos Aguas (Spain), Andilla (Spain), and Grammatico (Greece) – have been selected for this study. Fig. 1 shows an overview of the study areas including a composite of SAR pre- and post-disaster images. The fire scars for each scene are shown in red, whereas unburned areas appear in grey. The study site La Palma is not geographically located in the European Mediterranean, but shows comparative vegetation and landscape characteristics like the other study areas. The fires in La Palma occurred in the beginning of August 2009 in the south of the island and destroyed an area of approximately 2.200 ha. La Palma is characterized by a strong relief with steep slopes and an elevation ranging up to 1.900 m above sea level (a.s.l.). An area of approximately 1.300 ha was destroyed by forest fires in the region of Alto Trans-os-Montes located in the North of Portugal between the end of August 2011 and the beginning of September 2011. The Alto Trans-os-Montes region is marked by an undulating relief with elevations reaching from 400 m up to 1.150 m a.s.l.. Two fires near Valencia (Andilla and Dos Aguas) affected more than 36.000 ha. Both fires started at the end of June 2012 and lasted until the beginning of July 2012. The relief ranges from approximately 690 m – 1.320 m in Andilla and 100 m – 900 m in Dos Aguas. The fires in the study site Grammatico occurred at the end of August 2009, 30 km northeast of Athens and destroyed approximately 12.800 ha. Grammatico is characterized by a smooth terrain, ranging from 0 m to 500 m a.s.l.. All study areas are dominated by typical Mediterranean vegetation types (see Tab. 1) and a Mediterranean climate with dry and hot summers where the rainy season is concentrated around winter and spring.

3 Dataset

The dataset consists of five pairs of single-polarized horizontal transmitted and horizontal received (HH) TerraSAR-X images, acquired with the same acquisition parameters before and after forest fire occurrence. To consider the consequence of rainfall on the backscatter coefficient, TerraSAR-X scenes were ordered for dry as well as for wet environmental conditions. More detailed information on the datasets is given in Tab. 2. The SAR images were ordered in single-look slant-range complex (SSC), or enhanced ellipsoid corrected (EEC) format. The science orbit (TerraSAR-X 2012) was chosen for the highest orbital precision. The pre-processing was performed in six steps including multilooking (SSC data), co-registration, speckle filtering (Gamma-DE-MAP), geocoding, radiometric calibration and radiometric normalization using the SARscape 4.4 software (SARscape 2012). All data were converted to the radar backscatter coefficient sigma nought (dB).

Optical satellite images, CORINE 2006 land cover classification and precipitation information were collected and used as reference data. Post-disaster optical images were available for each study site. Furthermore, an optical pre-fire image was obtained for La Palma. Pre-processing steps applied to the optical images include orthorectification, pan-sharpening, atmospheric correction and co-registration to the TerraSAR-X images. The burned areas of all study sites were derived semi-automatically in the optical images. The classification workflow consists of an object-based procedure utilizing the indices modified soil adjusted vegetation index (MSAVI), burned area index (BAI) and normalized difference veg-

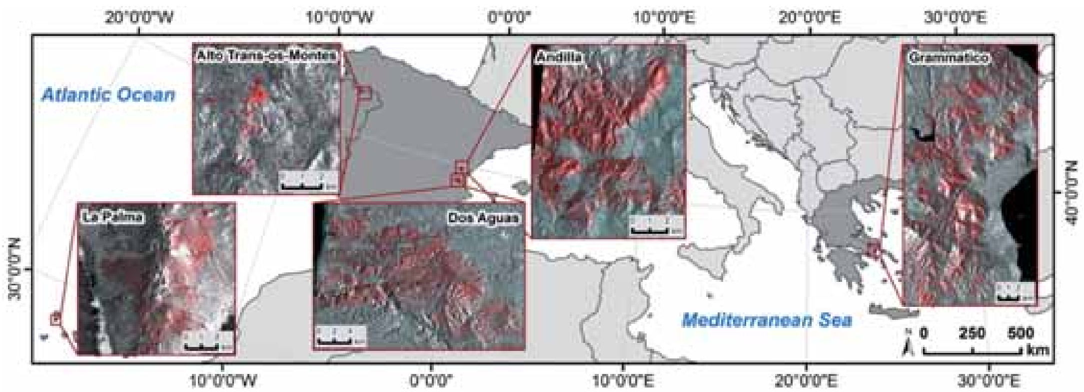

Fig. 1: Fire affected areas of the study sites are highlighted in red (RGB combination: red = change layer, green = pre-disaster image, blue = post-disaster image).

Tab. 1: Specification of CORINE 2006 land cover classification (CLC) (burned areas only).

Code	Vegetation class	Vegetation types
211	non-irrigated arable land	cereals, legumes, fodder crops, root crops and fallow land, tobacco, sugar cane; includes flowers and fruit trees (nurseries cultivation) and vegetables, whether open field, under plastic or glass (includes market gardening);
212	permanently irrigated land	crops irrigated permanently or periodically, using a permanent infrastructure (which is excluded in the class); most of these crops cannot be cultivated without an artificial water supply;
221	vineyards	areas planted with vines;
222	fruit trees and berry plantation	parcels planted with fruit trees or shrubs; single or mixed fruit species, fruit trees associated with permanently grassed surfaces; includes chestnut and walnut groves; ligneous crops, berry shrubs;
223	olive groves	areas planted with olive trees, including mixed occurrence of olive trees and vines on the same parcel;
231	pastures	dense grass cover, of floral composition, dominated by graminacea, not under rotation system; mainly for grazing, but the fodder may be harvested mechanically; includes areas with hedges; scattered trees and shrubs (10% - 20% of surface)
242	complex cultivation patterns	juxtaposition of small parcels of diverse annual crops, pasture and/or permanent crops; small parcels of annual crops (fruit trees, berry plantations, vineyards and olive groves), city garden pastures, fallow land;
243	land principally occupied by agriculture	areas principally occupied by agriculture, interspersed with significant natural areas; parcels of arable land, parcels of orchards, parcels of the rest of natural forests, groups of trees and shrubs (all smaller than 25 ha);
311	broad-leaved forest	vegetation formation composed principally of trees, including shrub and bush understoreys, where broad-leaved species predominate; young plantation of deciduous trees, walnut trees and chestnut trees, sparse broad-leaved forest with a 30% - 60% bracket of crown cover; quercus ilex, quercus suber, quercus rotondifolio;
312	coniferous forest	vegetation formation composed principally of trees, including shrub and bush understoreys, where coniferous species predominate; larch trees, arborescent mattoral with dominating Juniperus oxycedrus/phoenica;
313	mixed forest	vegetation formation composed principally of trees, including shrub and bush understoreys, where neither broad-leaved nor coniferous species predominate;
321	natural grassland	low productivity grassland; often situated in areas of rough, uneven ground; frequently includes rocky areas, briars and heathland; herbaceous vegetation; karstic areas, military training fields, areas of shrub formations of scattered trees;
322	moors and heathland	vegetation with low and closed cover, dominated by bushes, shrubs and herbaceous plants (heather, briars, broom, gorse, laburnum), dwarf forest with a 3 m maximum height, pinus mugo coverage, prostrate, box trees, gorse;
323	sclerophyllous vegetation	bushy sclerophyllous vegetation, includes maquis and garrigue; in case of shrub vegetation areas composed of sclerophyllous species, such as Juniperus oxycedrus and heathland species
324	transitional woodland shrub	bushy or herbaceous vegetation with scattered trees; can represent either woodland degradation or forest regeneration/recolonisation; e.g young broad-leaved and coniferous wood species with herbaceous vegetation
332	bare rock	scree, cliffs, rock outcrops, including active erosion, rocks and reef flats situated above the high-water mark; sparsely vegetated areas where 75% of the land surface is covered by rocks;
333	sparsely vegetated areas	includes steppes, tundra and badlands; scattered high-altitude vegetation, gramineous and/or ligneous and semi-ligneous species; e.g. Artemisia spp., Stipa spp.

Tab. 2: Available dataset.

Study site	Sensor	Date	Fire condition	Modus	Optical bands / polarization	Precipitation* Date / Amount	Inci-dence angle
Alto Trans-os-Montes	WorldView2 TerraSAR-X TerraSAR-X	28.8.2011 12.8.2011 3.9.2011	Post-fire Pre-fire Post-fire	- ScanSAR ScanSAR	coastal, blue, green, yellow, red, red-edge, NIR I, NIR II HH HH	-	- 27.7° 27.6°
Andilla	WorldView2 TerraSAR-X TerraSAR-X	6.7.2012 12.4.2012 9.7.2012	Post-fire Pre-fire Post-fire	- StripMap StripMap	coastal, blue, green, yellow, red, red-edge, NIR I, NIR II HH HH	1.7.2012 / 2.5 mm	- 37.2° 35.3°
Dos Aguas	WorldView2 TerraSAR-X TerraSAR-X	4.7./6.7.2012 21.3.2012 9.7.2012	Post-fire Pre-fire Post-fire	- StripMap StripMap	coastal, blue, green, yellow, red, red-edge, NIR I, NIR II HH HH	20.3.2012 / 58.9 mm 21.3.2012 / 4.8 mm	- 35.2° 35.3°
La Palma	SPOT5 SPOT5 TerraSAR-X TerraSAR-X	30.7.2007 7.8.2009 13.12.2007 9.8.2009	Pre-fire Post-fire Pre-fire Post-fire	- - StripMap StripMap	green, red, NIR, SWIR green, red, NIR, SWIR HH HH	-	- - 33.4° 33.4°
Grammatico	SPOT5 TerraSAR-X TerraSAR-X	25.8.2009 8.3.2009 31.8.2009	Post-fire Pre-fire Post-fire	- StripMap StripMap	green, red, NIR, SWIR HH HH	-	- 31.2° 31.2°

*www.wunderground.com (26.2.2013)

etation index (NDVI) in case a mid-infrared band was available. Additionally, all burned areas were screened and corrected by visual analysis. CORINE 2006 was created during 2005 – 2007 on the basis of SPOT4 VHR, SPOT5 VHR and IRS-P6-LISS-III data and reaches a classification accuracy of more than 85% (Büttner & Kosztra 2007). The minimum mapping unit for CORINE is 25 ha for a single vegetation type. Thus, areas covered by various vegetation types smaller than 25 ha are classified in mixed classes, e.g. complex cultivation patterns and land principally occupied with agriculture (Bossard et al. 2000). Tab. 1 specifies all vegetation types appearing in the burned scars of our study sites. For two study sites, Andilla and Dos Aguas, rainfall was observed recently before data acquisition took place. The corresponding meteorological data were collected from nearby meteorological stations, provided by the Spanish National Meteorological Agency (AEMET).

4 Methods

The authors analyzed the change of SAR backscatter coefficients caused by five forest fires (see section 3) and assessed if pre-fire vegetation types and density influence SAR backscatter behaviour. The obtained results were integrated in an enhanced SAR burned area classification algorithm. An accuracy assessment for the semi-automatically derived classification algorithm was performed. The flow chart of the proposed analysis scheme is shown in Fig. 2.

4.1 *SAR Backscatter Change Analysis*

The pre-processed SAR data (section 3) were intersected with CORINE 2006 land cover data. The burned and unburned parts of the image were defined using the optical derived reference data and subsequently averaged for each land cover type. Afterwards, the backscatter change values were computed by differencing the values of pre- and post-disaster data. Only vegetation classes of more than five ha were used.

The burned area of La Palma was investigated in more detail by calculating Pearson's correlation coefficients of the mean values of the normalized difference vegetation index (NDVI), the normalized difference shortwave infrared index (NDSWIR) and the SAR backscatter change values. For this purpose, the NDVI and NDSWIR values were grouped in 0.1 intervals. Only intervals containing a significant number of pixels ($p > 500$) were used, resulting in ranges from 0 to 0.8 (NDVI) and -0.1 to 0.6 (NDSWIR). These areas were intersected with the TerraSAR-X pre-disaster and post-disaster images. The NDVI and NDSWIR values were chosen as a proxy for vegetation density. A low index value corresponds to a low vegetation density. Contrarily, a high index value indicates a high vegetation density.

4.2 *SAR Classification and Accuracy Assessment*

The TerraSAR-X images have been classified by an object-based semi-automatic algorithm suited for rapid mapping activities for the Mediterranean Basin. The algorithm is based on SAR image change detection techniques (difference, ratio, normalized change index) in conjunction with a fuzzy classification approach and post-classification refinement. The method is described in more detail in Bernhard et al. (2011). Further, the obtained backscatter characteristics of each vegetation type were considered to enhance the classification algorithm. Thus, the thresholds for burned area detection were computed individually for each CORINE land cover type using the mean difference and the 90% quantile of the change values between pre- and post-disaster images.

To investigate if pre-fire vegetation types influence the classification accuracy, a detailed accuracy assessment was performed. The SAR classification result has been intersected with the reference burned area extent. Only areas which were correctly classified in the SAR as well as in the optical data were considered for the analysis. The SAR classification result was then intersected with CORINE land cover classification and the accuracy assessment was performed individually for each vegetation type.

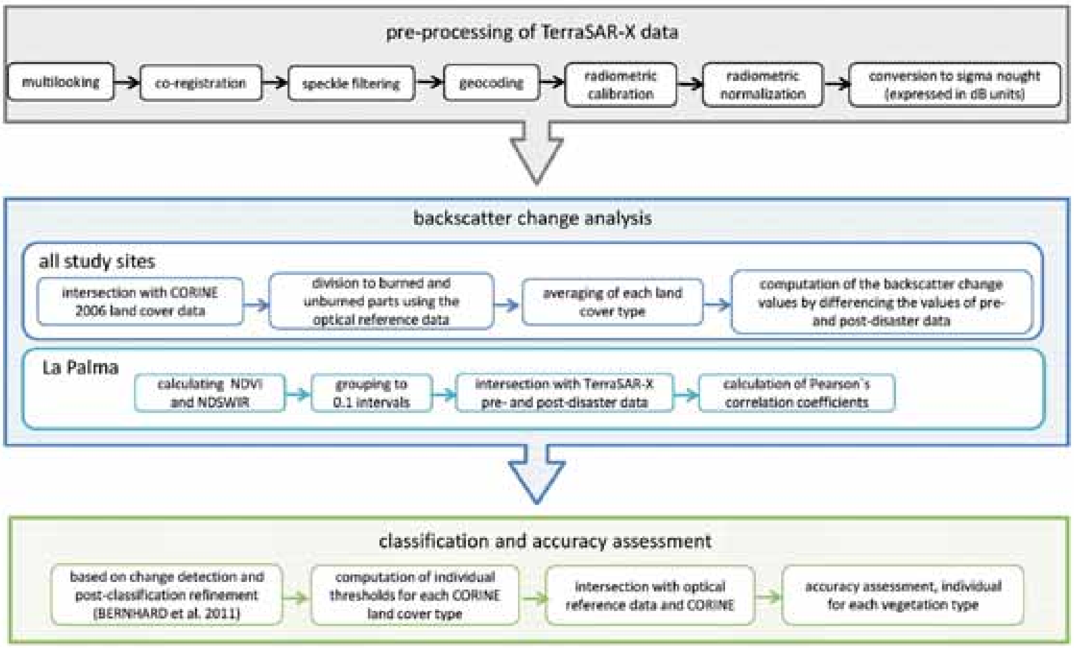

Fig. 2: Flow chart of pre-processing, backscatter change analysis, burned area classification and accuracy assessment of the TerraSAR-X data.

5 Results and Discussion

5.1 *SAR Backscatter Change Analysis*

The calculated pre- to post-disaster SAR backscatter difference coefficients (BDCs) are presented in Fig. 3. The figure illustrates the mean SAR backscatter change values for each CORINE land cover type, given for fire affected (Fig. 3a) as well as unaffected areas (Fig. 3b). First, the study sites observed under dry environmental conditions (La Palma, Alto Trans-os-Montes and Grammatico) are being discussed. Afterwards, the results of data acquired under wet conditions (pre- versus post-disaster) (see section 3), are being presented.

The study sites with dry acquisition conditions showed highest burned SAR BDCs for coniferous forest, transitional woodland shrub and moors and heathland. This can be attributed to tall and dense vegetation growth previous to burning, a decreased attenuation in the canopy due to the consumption of the needles or leaves by the fire, strong trunk-ground interactions (double-bounce), and an exposal of a rough ground surface. Lowest SAR BDC values in fire affected areas could be obtained for non-irrigated arable land (Grammatico), vineyards (La Palma), complex cultivation patterns (Grammatico) and land principally occupied by agriculture (Grammatico, Alto Trans-os-Montes). No significant change (all values were within the relative radiometric accuracy of TerraSAR-X of 0.7 dB (Eineder et al. 2009) of burned SAR BDCs was observed in sclerophyllous vegetation present in La Palma and pastures and vineyards in Grammatico. The low values can be explained by scant vegetation (see also Tab. 1) causing no significant change in backscatter, or low fire severities. The SAR BDCs for unburned areas were rather constant in time, and did not exceed the relative radiometric accuracy of TerraSAR-X (Eineder et al. 2009), except for non-irrigated arable land in Alto Trans-os-Montes. A possible explanation could be changes in agricultural management.

Rainfall before post-disaster image acquisition in the study site of Andilla (see Tab. 2) implied an increase in soil and vegetation moisture. Thus, highest SAR BDCs could be obtained for burned as well as for unburned areas, whereas the increase of SAR BDCs for areas unaffected by fire was lower (around 1.7 dB) than the SAR BDCs for areas affected by fires (up to 7.4 dB). The SAR BDCs in comparison with the results obtained under dry conditions showed an increase of 1.5 dB – 2.3 dB in unburned and 2.2 dB – 6.1 dB in burned areas. These values are confirmed by Tanase et al. (2010c), who observed that the effect of rainfall during summer season increases SAR BDCs from around 1 dB (unburned forest) up to 6 dB (burned area). But, regardless of rainfall, Andilla showed the same trend as the study sites unaffected by rainfall, with highest SAR BDCs associated with tall and dense vegetation structure, whereas vegetation classes with lower SAR BDCs include scant and lower growing vegetation (see Tab. 1).

The second study site affected by rainfall was Dos Aguas. In contrast to Andilla the rainfall occurred prior to the pre-disaster image acquisition and implied higher backscatter coefficients in the pre-disaster image in tall and dense vegetation (up to -8.8 dB versus -13.0 dB in Andilla) than in scant vegetation (up to -11.0 dB versus -11.0 dB in Andilla). This consequently influenced the SAR BDCs. Thus, dense vegetation achieved low SAR BDC values (burned areas up to 1.7 dB and unburned areas up to 1.4 dB), and sparsely growing vegetation obtained high (burned areas up to 3.5 dB and unburned areas up to 1.4) SAR BDC values in comparison to the other study sites.

The scatter plots obtained for La Palma are illustrated in Fig. 4. The results confirmed the previously observed relationship between fire-related backscatter changes and pre-fire vegetation characteristics. SAR BDC values for burned areas versus pre-fire NDVI and NDSWIR values showed a strong positive correlation with $R_{NDVI} = 0.94$ and $R_{NDSWIR} = 0.98$, indicating a clear positive relationship between SAR BDCs and vegetation indices. The correlation showed that low pre-fire vegetation density led to low SAR BDCs, and, vice versa, high pre-fire vegetation density implied high SAR BDCs.

5.2 *SAR Classification Accuracy*

The results of the SAR classification in comparison to the combined dataset of the optically derived burned area and CORINE 2006 data are illustrated in Tab. 3. Study sites not affected by precipitation reached highest classification accuracies for coniferous forest (86%, 89%, 91%), and lowest for pastures (5%, 17%). Data acquired under wet conditions (post-dis-

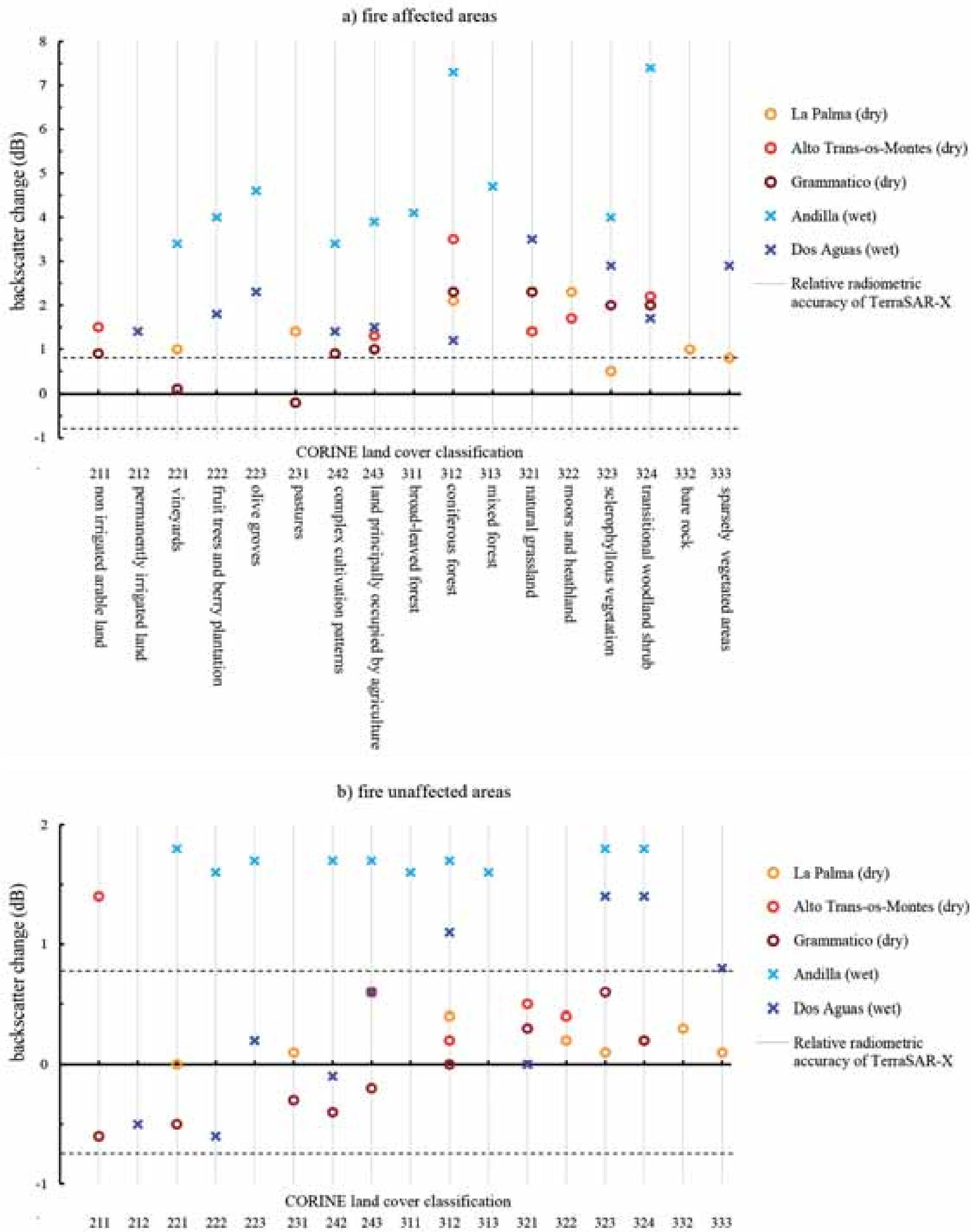

Fig. 3: SAR backscatter difference coefficients versus CORINE vegetation classes for a) fire affected and b) fire unaffected areas. Dry study sites are marked by a circle and wet acquisition conditions by a cross.

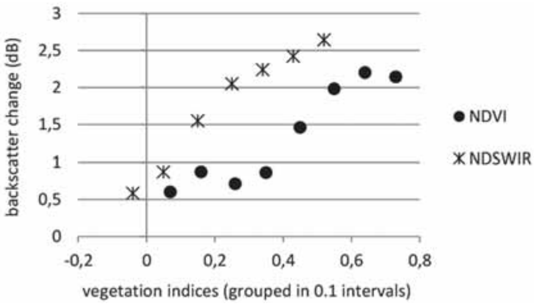

Fig. 4: Scatter plot NDVI and NDSWIR versus SAR BDCs in La Palma.

aster) showed highest values for mixed and coniferous forest (81%, 78%), and a lowest value for complex cultivation patterns (39%). The achieved results indicated, that high accuracy values were linked to tall and dense vegetation (see Tab. 1), whereas sparse vegetation exhibited a reduced accuracy, and confirmed the obtained trend of the SAR BDCs analysis. A similar trend was observed by Mari et al. (2012), who used L-band data for damage assessment in Sardinia. Wet conditions in the pre-disaster image led to highest accuracies for natural grassland (86%) and sparsely vegetated areas (86%), where lowest accuracy has been obtained for permanently irrigated arable land (33%). Precipitation prior to pre-disaster image acquisition did not determine lower accuracy values, but an inverse trend could be observed. High accuracies could be obtained in sparsely growing, and comparably low accuracies in dense vegetation.

6 Conclusion

In the framework of this study SAR backscatter coefficients and classification accuracy related to pre-fire vegetation type and density have been analyzed. The study was assessed for five study sites located at La Palma, Alto Trans-os-Montes, Dos Aguas, Andilla and Grammatico, and considered dry as well as wet environmental conditions.

Tab. 3: Classification result of the SAR burned area algorithm in %.

CLC-code	Vegetation class	La Palma	Alto Trans-os-Montes	Dos Aguas	Andilla	Grammatico
211	non-irrigated arable land		27			69
212	permanently irrigated land			33		
221	vineyards	50			42	76
222	fruit trees and berry plantation			44	56	
223	olive groves			48	69	
231	pastures	5				17
242	complex cultivation patterns			39	39	44
243	land principally occupied by agriculture		28	54	55	75
311	broad-leaved forest				58	
312	coniferous forest	89	86	55	78	91
313	mixed forest				81	
321	natural grassland		42	86		79
322	moors and heathland	32	51			
323	sclerophyllous vegetation	12		83	65	69
324	transitional woodland shrub		74	72	66	77
332	bare rock	29				
333	sparsely vegetated areas	40		86		

SAR backscatter difference coefficients (BDCs) were analyzed for correlations to CORINE 2006 land cover data. The results pointed out that highest SAR BDCs were linked to tall and dense pre-fire vegetation, whereas scant vegetation was marked by lowest differences. This trend was observed in dry as well as in wet environmental conditions when rainfall occurred before the post-disaster image acquisition. Precipitation prior to pre-disaster image acquisitions led to an inverse trend.

A regression analysis of the SAR BDCs, the NDVI and the NDSWIR values for La Palma showed positive correlations. The vegetation indices were used as a proxy for vegetation density, and the correlation coefficients approved the previous obtained relationship between pre-fire vegetation structure and SAR BDCs of dry and wet (post-disaster) environmental conditions.

A classification and accuracy assessment of the proposed algorithm was performed using the optical derived burned area extent as a reference. Since the thresholds for burned area classification were computed individually for each vegetation type, individual class accuracies of up to 91% could be obtained. Nevertheless, classification accuracies (5% – 91%) varied strongly according to the individual (low versus dense) vegetation type.

The lack of ground truth data led to an estimation of vegetation density by vegetation indices. Ground truth data would be necessary to investigate the obtained relationship between pre-fire vegetation density, soil moisture, fire severity and SAR BDCs in more detail. Moreover, it is of interest whether tree crowns stay possibly unaffected by fire. This would lead to an unchanged backscatter behaviour for X-band data, although the ground vegetation might be completely burned. A comparison to other microwave bands (such as L-band) could help to understand SAR backscatter behaviour after forest fires in more detail, and show the potential strengths and weaknesses of each method applied. The results presented are valid for most vegetation types occurring in the European Mediterranean. In significantly different environments, such as tropical or boreal forests, other trends might be observed.

Our analysis confirmed the applicability of X-band SAR data for burned area mapping in the European Mediterranean. According to this finding, fire management might profit from a more extensive or complementary use of SAR data for burned area detection, especially under challenging weather conditions.

References

Amraoui, M., DaCamara, C. & Pereira, J., 2010: Detection and monitoring of African vegetation fires using MSG-SEVIRI imagery. – Remote Sensing of Environment **114** (5): 1038–1052.

Bernhard, E., Twele, A. & Gähler, M., 2011: Rapid Mapping of Forest Fires in the European Mediterranean Region – a Change Detection Approach Using X-Band SAR Data. – PFG –Photogrammetrie, Fernerkundung, Geoinformation **2011** (4): 261–270.

Bossard, M., Feranec, J. & Otahel, J., 2000: Corine land cover technical guide. – Addendum 2000, European Environment Agency, technical report No. 4.

Bourgeau-Chavez, L., Harrell, P., Kasischke, E. & French, N., 1997: The detection and mapping of Alaskan wildfires using a spaceborne imaging radar system. – International Journal of Remote Sensing **18:** 355–373.

Bourgeau-Chavez, L., Kasischke, E., Brunzell, S., Mudd, J. & Tukman, M., 2002: Mapping fire scars in global boreal forests using imaging radar data. – International Journal of Remote Sensing **23** (20): 4211–4234.

Büttner, G. & Kosztra, B., 2007: CLC2006 Technical Guidelines. – European Topic Centre, European Environment Agency, Spain.

Eineder, M., Fritz, T., Mittermayer, J., Roth, A., Börner, E. & Breit, H., 2009: TerraSAR-X Ground Segment Basic Product Specification Document. – Cluster applied remote sensing, German Aerospace Center (DLR), Wessling.

French, N., Kasischke, E., Bourgeau-Chavez, L. & Harrell, P., 1996: Sensitivity of ERS-1 SAR to variations in soil water in fire-disturbed boreal forest ecosystems. – International Journal of Remote Sensing **17:** 3037–3053.

Gimeno, M., San-Miguel Ayanz, M. & Liberta, G., 2003: Fire scar detection in central Portugal using RADARSAT-1 and ERS-2 SAR data. – IEEE International Geoscience and Remote Sensing Symposium **I-VII:** 2491–2493.

Gimeno, M. & Ayanz, J., 2004a: Evaluation of Radarsat-1 data for identification of burnt areas in southern Europe. – Remote Sensing of Environment **104:** 346–359.

Gimeno, M., San-Miguel-Ayanz, J. & Schmuck, G., 2004b: Identification of burnt areas in Mediterranean forest environments from ERS-2 SAR time series. – International Journal of Remote Sensing **25** (22): 4873–4888.

Hoekmann, D., 1987: Measurements of the Backscatter and Attenuation Properties of Forest Stands at X-, C- and L-Band. – Remote Sensing of Environment **23:** 397–416.

Justice, C.C. & Koronzti, S., 2001: A review of the status of satellite fire monitoring and the requirements for global environmental change research. – Ahern, F. (ed.): Global and regional vegetation fire monitoring from space: planning a coordinated international effort: 1–19.

Justice, C., Giglio, L., Koronzti, S., Owens, J., Morisette, J., Roy, D., Desdoitres, J., Alleaume, S., Petitcolin, F. & Kaufman, Y., 2002: The MODIS fire products. – Remote Sensing of Environment **83** (1–2): 244–262.

Karszenbaum, H., Tiffenberg, J., Grings, F., Marinez, J., Kandus, P. & Pratolongo, P., 2003: A SAR time series analysis toolbox for extracting fire affected areas in wetlands. – IEEE Geoscience and Remote Sensing Symposium, IGARSS ‘03 **6:** 4107–4109.

Kasischke, E., Bourgeau-Chavez, L., French, N., Harrell, P. & Christensen, N., 1992: Initial observations on using SAR to monitor wildfire scars in boreal forests. – International Journal of Remote Sensing **13** (18): 3495–3501.

Leone, V., 2009: Human factors of fire occurrence in the Mediterranean. – Chuvieco, E. (ed.): Earth observation of wildland fires in Mediterranean ecosystems, Springer: 149–179.

Margaris, N., Koutsidou, E. & Giourga, C., 1996: Changes in traditional Mediterranean land-use systems. – Brandt, C. & Thornes, J. (eds.): Mediterranean desertification and land use, 1996.

Mari, N., Laneve, G., Cadau, E. & Porcasi, X., 2012: Fire Damage Assessment in Sardinia: the use of ALOS/PALSAR data for post fire effects management. – European Journal of Remote Sensing **45:** 233–241.

Menges, C., Bartolo, R., Bell, D. & Hill, G., 2004: The effect of savanna fires on SAR backscatter in northern Australia. – International Journal of Remote Sensing **25** (22): 3857–4871.

Pulliainen, J., Heiska, K., Hyyppä, J. & Hallikainen, M., 1993: Backscattering Properties of Boreal Forests at the C- and X-Bands. – IEEE Geoscience and Remote Sensing Symposium **2:** 388–390.

SARscape, 2012: SARscape® 4.4, system for optical and SAR image analysis, Cascine di Barico, Purasca, Switzerland.

Siegert, F. & Rücker, G., 2000: Use of multitemporal ERS-2 SAR images for identification of burned scars in south-east Asian tropical rainforest. – International Journal of Remote Sensing **21** (4): 831–837.

Tanase, M., Pérez-Cabello, F., Riva, J. & Santoro, M., 2010a: TerraSAR-X data for burn severity evaluation in Mediterranean forests on sloped terrain. – IEEE Transactions on Geoscience and Remote Sensing **48** (2): 917–929.

Tanase, M., Santoro, M., Wegmüller, U., de la Riva, J. & Pérez-Cabello, F., 2010b: Properties of X-, C- and L-band repeat-pass interferometric SAR coherence in Mediterranean pine forests affected by fires. – Remote Sensing of Environment **114:** 2182–2194.

Tanase, M., Santoro, M., de la Riva, J., Pérez-Cabello, F. & Toan, T., 2010c: Sensitivity of X-, C-, and L-Band SAR Backscatter to Burn Severity in Mediterranean Pine Forests. – IEEE Transaction geoscience and remote sensing **48** (10): 3663–3675.

TerraSAR-X, 2012: TX-GS-PL-4001. – https://www.terrasar-x.dlr.de/pdfs/TX-GS-DD-3302.pdf (11.12.2012).

Viegas, D., Ribeiro, L., Viegas, M., Pita, L. & Rossa, C., 2009: Impacts on fire on society: extreme fire propagation issues. – Chuvieco, E. (ed.): Earth observation of wildland fires in Mediterranean ecosystems, Springer: 97–109.

Wastl, C., Schunk, C., Leuchner, M., Pezzatti, G. & Menzel, A., 2012: Recent climate change: long-term trends in meteorological forest fire danger in the Alps. – Agricultural and forest meteorology **162–163:** 1–13.

Address of the Authors:

Eva-Maria Bernhard, André Twele & Sandro Martinis, German Aerospace Center (DLR), German Remote Sensing Data Center (DFD), D-82234 Oberpfaffenhofen, Tel.: +49-(0)8153-28-2481, -3510, -3034, Fax: +49-(0)8153-28-1445, e-mail: {eva-maria.bernhard}{andre.twele}{sandro.martinis}@dlr.de

Manuskript eingereicht: Februar 2014
Angenommen: April 2014